A Medium-Frequency Transformer with Multiple Secondary Windings for Grid Connection through H-Bridge Voltage Source Converters

Md Rabiul Islam, Youguang Guo and Jianguo Zhu
Faculty of Engineering and Information Technology, University of Technology Sydney, NSW 2007, Australia
Md.Islam@uts.edu.au, Rabiulbd@hotmail.com

***Abstract*--Although the power output of today's wind turbine has exceeded 7 MW, the voltage rating of the most common generator is below 700 V. A low-frequency transformer is commonly used to step-up the voltage to the grid voltage level, e.g. 11 kV or 33 kV. These heavy and bulky low-frequency transformers significantly increase the volume and weight of nacelle. To achieve a compact and light nacelle, a medium-voltage converter with series-connected H-bridge (SCHB) topology would be an attractive technology for future wind turbines. However, the SCHB converter requires multiple isolated and balanced DC sources, which makes the application not straightforward. As an alternative approach to generate multiple isolated and balanced sources a prototype transformer with six secondary windings, 1.26 kVA and 10 kHz, is designed and developed for 1 kV five levels SCHB multilevel converters. The experimental results show that the proposed system may be attractive in grid based renewable energy systems.**

***Index Terms*--Direct grid connection, medium-voltage converter, medium-frequency transformer-link, wind turbine.**

I. Introduction

Larger size wind turbines are able to generate more electricity at lower cost compared to the smaller turbines. This is because the set-up costs and maintenance costs do not depend on the size of the machine; almost constant when machine size changes. Due to this interest, the output power of today's wind generators has exceeded 7 MW. For example, since 2011 ENERCON has been producing wind turbine E-126/7500 with a power capacity of 7.5 MW [1]. Currently Sway Turbine and Windtec Solutions are developing 10 MW wind turbine generators, which are expected to be commercially available by 2015 [2], [3].

TABLE I
Wind Turbine Generator Voltage Rating

Turbine Power (MW)	Voltage (V)	Model	Manufacturer
1.5	575	1.5_{SLE}	GE Energy
1.65	690	Wt1650	Windtec
2.05	575	MM92	REpower
3	400	E-82 E3	ENERCON
5	690	Bard 5.0	Bard Engineering
5.5	690	Wt5500	Windtec
10	690	SeaTitan	Windtec

Although the power rating of wind generators has been increasing rapidly, the voltage rating of the most common generators is below 700 V. Table I summarizes the voltage ratings of different wind turbine generators [3]-[7]. Therefore, converter voltage level is also below 700 V due to the lower generator voltage rating and the use of two-level converter topology. To reduce the electrical losses, a low-frequency power-transformer is commonly used to step-up the voltage to grid voltage level as shown in Fig. 1. There are several special transformers commercially available for wind turbine systems, like vacuum cast coil, SLIM and liquid-filled. Although new designs aim to reduce the transformer size and weight but still the transformers are heavy and bulky for wind turbine systems. The weight and volume of a 33/0.69 kV, 2.6 MVA transformers is typically in the range of 6 ~ 8 tons and 5 ~ 9 m^3 respectively [8], [9]. This heavy and bulky low-frequency transformer significantly increases the weight and volume of nacelle as well as the mechanical stress of the tower.

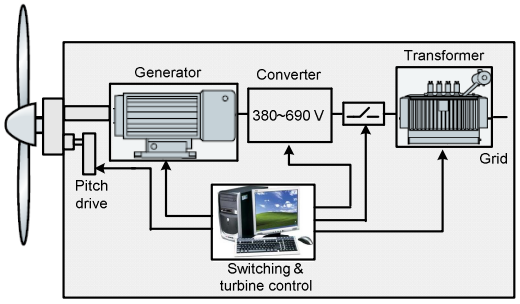

Fig. 1. Conventional wind turbine system.

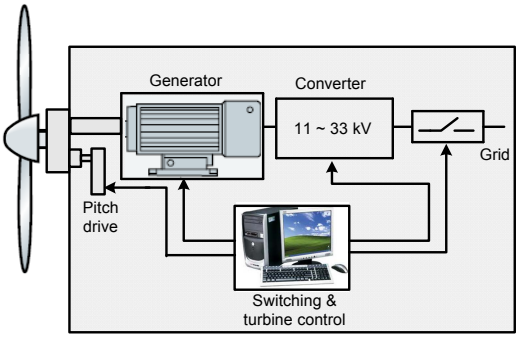

Fig. 2. Medium-voltage converter based wind turbine system.

Hence, a transformer-less, medium-voltage converter based nacelle would be an attractive technology for the future wind turbines. Fig. 2 shows the medium-voltage converter based wind turbine system.

With the arrival of new high-power semiconductor devices, new power converter structures are conceived to

meet the needs of future medium or high-voltage converter systems. In this highly active area, neutral point clamped (NPC), flying capacitor (FC) and series connected H-bridge (SCHB) converter topologies and circuits have found their application in low voltage systems [10], [11]. For medium or high-voltage applications, however, the selection of multilevel converter topology is very critical. The component numbers of NPC and FC converters scale quadratically with the number of levels. Also, the voltage balancing becomes a significant problem for high-level numbers [12]. The component numbers of the SCHB converters scale linearly with the number of levels and the individual modules are identical and completely modular in construction and hence enable high-level number attainability. High-level converter implies elimination of power transformer and lower total harmonic distortion (THD) with lower switching frequency, eliminating the output filters and reducing running cost [13]. High-level number attainability also allows lower level of DC link voltage requirement for each H-bridge cell that eliminates boosters. Moreover, in the case of a fault in one of these modules, it is possible to replace it quickly and easily. A comparative study among these three multilevel converter topologies has been carried out. Based on performance, complexity and cost, the SCHB topology has gained highest index value for their medium or high-voltage applications [14]. However, the SCHB converter requires multiple-isolated DC sources that must be balanced as shown in Fig. 3, and therefore its application is not straightforward, especially in wind generation systems. Many researchers are addressing their efforts in proposing special modulation techniques [15], switched DC voltage sources and low-frequency transformer feeding [16]. The first two approaches do not give overall solution and the third introduces a complicated three phase heavy and bulky transformer. Recently a high-frequency link was proposed for asymmetrical cascaded H-bridge (ACHB) inverter [17]. The main H-bridges are supplied in parallel by the single DC source, so the application of this approach is limited only to the isolated winding motor loads.

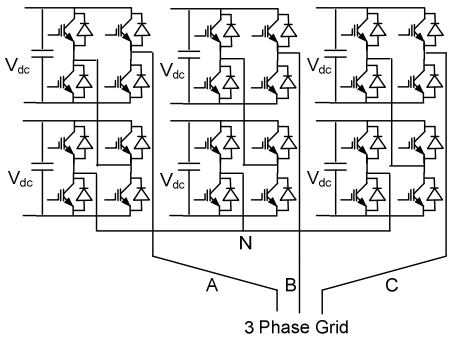

Fig. 3. Three-phase five-level SCHB multilevel converter.

A new type of modular permanent magnet wind generator with a large number of isolated coils has been proposed to generate independent sources for SCHB medium voltage converter [18]. This multi-windings generator requires a special winding arrangement as well as complicated control strategies. Moreover, this approach does not work with the existing wind generators. The general concept of a novel medium-voltage SCHB multilevel converter system was proposed to eliminate the grid-side step-up transformer, which is desirable for both onshore and offshore wind turbines [19].

In this paper a medium-frequency transformer-link is designed and developed to generate the isolated balanced multiple DC supplies for the SCHB converter from a single low-voltage commercially available classical generator. The advantages of this medium-frequency transformer-link for medium-voltage converter based wind turbine are: (i) no requiring special generator or phase-shifted transformer (ii) inherent DC-link voltage balancing due to single DC supply, (iii) compact and light overall system, and (iv) simple installation and low maintenance cost. In this paper a prototype transformer with six secondary windings, 1.26 kVA and medium frequency, is designed and developed for 1 kV five levels SCHB multilevel converters. The specification for the transformer is summarized in Table II. The details design process and experimental results are addressed in the following sections.

TABLE II
SPECIFICATIONS OF THE TRANSFORMER

Number of primary windings	1
Number of secondary windings	6
Switching frequency	10 kHz
Primary windings voltage	210 V
Secondary windings voltage	374 V
Power rating	1.26 kVA

II. TRANSFORMER DESIGN

The increase on operating frequency contributes to volume and weight reduction and therefore, transformer material is economized. With the advent of new power semiconductor devices, different soft magnetic materials with high magnetic saturation flux density and low specific core loss, are conceived to reduce the weight and volume of conventional power transformers. However, special consideration is essential to create optimal energy transfer since the behavior of a transformer can significantly change as frequency increases due to redistribution of magnetic field and current density within the conductors. Moreover, the transformer works with a square wave excitation voltage, so it needs a different design since a triangular flux is required to generate the square wave voltage.

A. Core Material Selection

Several types of magnetic core materials are commercially available for medium-frequency transformer. The ferrite material has gained popularity due to its price and availability, but it has very low saturation flux density in between 0.3 to 0.5 T which makes the transformer bulky especially for high-voltage and high-frequency systems. Silicon steel is one of the soft magnetic materials which have high saturation flux density of around 1.5 T and good permeability. Compared with other soft magnetic materials like

amorphous and nanocrystalline, its specific core loss is very high. An amorphous alloy based soft magnetic material is called Metglas, which has not only high permeability but also high saturation flux density of 1.56 T. The specific core loss of Metglas amorphous alloy is much lower than silicon steel but higher than that of nanocrystalline. The nanocrystalline has high saturation flux density of around 1 T and extremely low specific core loss. Although it has very low specific core loss the insulation issue and cost makes it unpopular especially for toroidal cores. Considering the flux density, specific core loss, cost and availability a Metglas 2506SA1 soft magnetic material with saturation flux density of 1.56 T and specific loss of 0.6 kW/kg can be chosen as the core material.

B. Turns Ratio Calculation

By Faraday's law, the voltage, v and flux, φ of a transformer can be related by

$$v(t) = N\frac{d\varphi}{dt} \tag{1}$$

where N is the number of turns.

The transformer works with a square wave voltage, so according to (1), a triangular flux is required to generate the square wave voltage as shown in Fig. 4, where T is the period of excitation voltage, V_{max} is the maximum excitation voltage, and φ_{max} is the maximum flux.

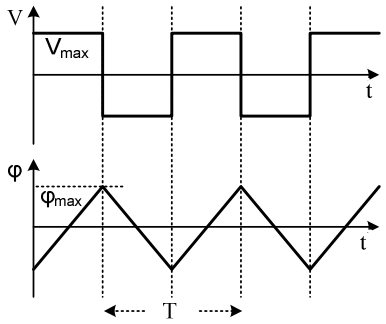

Fig. 4. Voltage and flux in a square wave transformer.

The triangular flux can be modeled mathematically as

$$\varphi(t) = \begin{cases} \frac{\varphi_{\max}}{T/4}(t-\frac{T}{4}).....0 \le t \ge \frac{T}{2} \\ \frac{-\varphi_{\max}}{T/4}(t-\frac{3T}{4}).....\frac{T}{2} \le t \ge T \end{cases} \tag{2}$$

The expression of voltage can be deduced by (1) and (2) as

$$v(t) = \begin{cases} N\frac{\varphi_{\max}}{T/4}.....0 \le t \ge \frac{T}{2} \\ -N\frac{\varphi_{\max}}{T/4}.....\frac{T}{2} \le t \ge T \end{cases} \tag{3}$$

If

$$V_{\max} = N\frac{\varphi_{\max}}{T/4} \tag{4}$$

then (3) can be modified as

$$v(t) = \begin{cases} V_{\max}.....0 \le t \ge \frac{T}{2} \\ -V_{\max}.....\frac{T}{2} \le t \ge T \end{cases} \tag{5}$$

Expression (4) is the mathematical model of excitation voltage waveform as shown in Fig. 4. The rms value of excitation voltage can be calculated as

$$V_{rms} = \sqrt{\frac{1}{T}\left\{V_{\max}^2\left(\frac{T}{2}\right) + (-V_{\max})^2\frac{T}{2}\right\}}$$

$$V_{rms} = \sqrt{\frac{1}{T}\left\{2V_{\max}^2\left(\frac{T}{2}\right)\right\}}$$

$$V_{rms} = V_{\max} \tag{6}$$

If f is the frequency of the excitation voltage, B_{max} is the maximum flux density and A is the cross-section area of the transformer core, then from (4) and (6) the expression of number of turns can be deduce as

$$V_{rms} = V_{\max} = N\frac{\varphi_{\max}}{T/4}$$

$$= 4 \cdot f \cdot N \cdot \varphi_{\max}$$

$$= 4 \cdot f \cdot N \cdot B_{\max} \cdot A$$

$$\therefore N = \frac{V_{rms}}{4 \cdot f \cdot B_{\max} \cdot A} \tag{7}$$

If the transformer excitation frequency is 10 kHz, core size is 5 cm^2 (2.5 cm × 2 cm) and the flux density is 1 T, then the minimum number of turns required by the primary of the transformer can be calculated using:

$$N_p = \frac{V_{rms(pri)}}{4 \cdot f \cdot B_{\max} \cdot A}$$

$$= \frac{210}{4 \cdot 10 \times 10^3 \cdot 1 \cdot 5 \times 10^{-4}}$$

$$= 10.50$$

and each secondary winding minimum required number of turns can be calculated using:

$$N_s = \frac{V_{rms(sen)}}{4 \cdot f \cdot B_{\max} \cdot A}$$

$$= \frac{374}{4 \cdot 10 \times 10^3 \cdot 1 \cdot 5 \times 10^{-4}}$$

$$= 18.70$$

Finally, the design is considered 14 turns for primary windings and 25 turns for each secondary winding.

C. Wire Selection

With the increase of excitation frequency the current density will be reduced inside the conductor and increased in the surface; this is called the skin effect. Although the total current in the conductor will not suffer by skin effect, the current density will become non-uniform. This property of conducting materials is also

known as skin depth, and which is defined as the radial distance from the surface of the conductor where the value of the current density is 37 % smaller than its value in the surface. Fig. 5 shows the effect of excitation frequency on conductor current distribution.

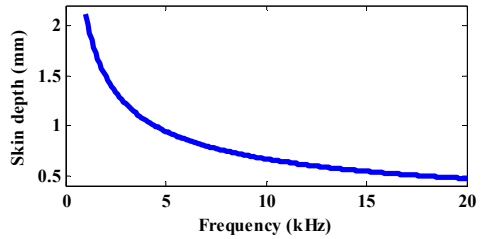

Fig. 5. Skin-depth versus excitation frequency of copper conductor.

On the other hand, the AC current in a wire, generates a magnetic field that enters adjacent conductors and induces voltages on them, resulting in additional current in the conductor; this is called proximity effect which highly depend on excitation frequency. Although the total current of the conductor does not change; the current density in the conductor will be reduced near the adjacent wire and reinforced in the opposite side e.g. redistribution of current density.

These two effects will increase the AC losses in high frequency windings. Special type of wire is conceived named Litz wire: a conductor consisting of insulated strands twisted or braided together. Such design equalizes the flux linkages of individual strands causing the current to spread uniformly throughout the conductor, e.g. the AC to DC resistance ratio tends to approach unity. The size of transformer winding copper wire depends on primary and secondary side current (i_p and i_s), e.g. 6 A and 1 A respectively. Current density, J is chosen as 4 A/mm^2, should be the appropriate for frequency of 10 kHz. The number of strands for primary and secondary winding wires can be assumed 13 and 3 respectively.

The minimum required cross section area of primary winding single strand can be calculated using:

$$a_p = \frac{\frac{i_p}{13}}{J} = 0.115 mm^2$$

and single strand diameter can be calculated using:

$$d_p = \sqrt{\frac{4 \cdot a_p}{\pi}} = 0.383 \text{ mm}$$

Also, the minimum required cross section area of secondary winding single strand can be calculated using:

$$a_s = \frac{\frac{i_s}{3}}{J} = 0.083 mm^2$$

and single strand diameter can be calculated using:

$$d_s = \sqrt{\frac{4 \cdot a_s}{\pi}} = 0.325 \text{ mm}$$

Finally, the same size strand is considered for both primary and secondary windings Litz wires with a diameter of 0.4 mm.

D. Core Size Selection

Theoretically the overall area of 13 strands wire is 1.638 mm^2. Practically, when the 13 insulated strands are twisted or braided together, the overall diameter of the Litz wire is 2 mm and the cross section area of the primary winding wire is 3.2 mm^2. On the other hand, theoretically the overall area of secondary windings of 3 strands wire is 0.378 mm^2. Practically, when the 3 insulated strands are twisted or braided together, the overall diameter of the Litz wire is 1 mm and the cross section area of the secondary winding wire is 0.79 mm^2.

Hence, the design can be considered as: the Litz wire cross section area of 4 mm^2 and 1.2 mm^2 for primary and secondary windings respectively. The area required by the primary and secondary windings, A_w is:

$$A_w = ((14 \times 4) + 6 \times (25 \times 1.2))$$
$$= 236 \text{ mm}^2$$

Considering a hole reserve factor of 8 for all the windings, the minimum required hole area should be 1888 mm^2 or 18.88 cm^2 and the hole diameter should be more than 4.7 cm. Finally, 6.5 cm inner diameter (ID), 10.5 cm outer diameter (OD) and 2.5 cm height (HT) are considered for the design. The dimensions of the core are shown in Fig. 6.

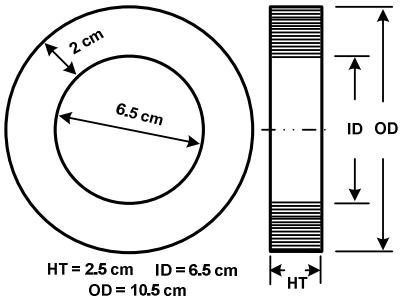

Fig. 6. Transformer core dimensions.

III. Prototype and Test Results

Metglas amorphous alloy 2605SA1 with 25 mm width and 30 µm thickness sheet and with saturation flux density of 1.56 T and specific losses of 0.6 kW/kg is used to develop the transformer core. The Metglas sheet was stacked in a frame with Araldite on the surface of each layer. During the stacking process equal and sufficient force was applied to make uniform distribution of Araldite. The photograph of the developed core is shown in Fig. 7. Designed Litz wires are used for primary and secondary windings. A photograph of the prototype transformer is shown in Fig. 8.

Average length of each turn is 0.13 m. Since the primary winding has 14 turns and each secondary winding has 25 turns, the total winding wire lengths for the primary and secondary windings are 1.82 m and 3.25 m respectively. About 0.14 m and 0.08 m extra wires are required for the end connection of primary and secondary winding respectively. When the strands are twisted together, the length of developed Litz wire should be shorter than strand's length. It is observed about 1.14 % and 1.09 % reduction of length in primary and secondary windings wires respectively.

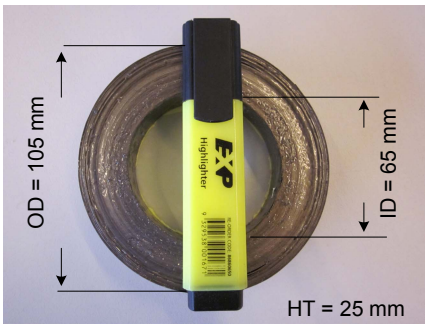

Fig. 7. Photograph of the developed core.

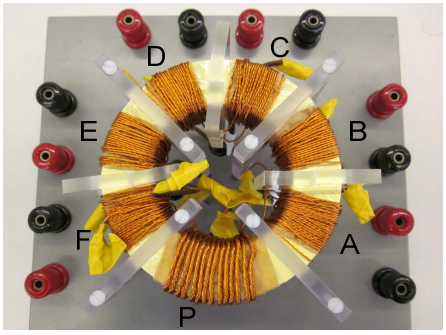

Fig. 8. Photograph of the prototype transformer.

Therefore, actual conductor length, L can be calculated as

$$L_p = (1.82 + 0.14) \times 1.14$$
$$= 2.24m$$

and

$$L_s = (3.25 + 0.08) \times 1.09$$
$$= 3.62m$$

If ρ is the copper specific resistivity, A_c is the cross-sectional area of the individual strand then individual strand resistance of primary and secondary windings can be calculated from

$$R = \rho \frac{L}{A_c}$$

Considering the temperature effect, the overall DC resistances of primary and secondary windings Litz wires are calculated as 0.0233 Ω and 0.162 Ω respectively.

Wheatstone bridge is used to measure the resistance of primary windings, P and all secondary windings, $A \sim F$, since windings resistances are very small. The leading wire resistance is also considered and subtracted from the measured values as summarized in Table III. The winding resistances measured are compared with theoretical values and the variation in percentage is also summarized in Table III.

Medium frequency performance has been analyzed in the laboratory. Medium frequency (e.g. 1 ~ 12 kHz) square wave signal is generated using GFG-8015G function generator and amplified by AM1600 Australian monitor power amplifier. The theoretical voltage transformation ratio is calculated as 1.781. The voltage transformation ratios of all secondary windings are also calculated. The measured ratios have been compared with the theoretical values and summarized in Table IV. The ratios are highly consistent with the theoretical values; this is important for the SCHB converter system.

TABLE III
WINDINGS DC RESISTANCES IN Ω

	P	A	B	C	D	E	F
Total	0.043	0.191	0.190	0.205	0.185	0.182	0.182
Leading wires	0.019	0.029	0.029	0.029	0.029	0.029	0.029
Windings	0.024	0.163	0.161	0.176	0.156	0.153	0.153
Variation (%)	+3	+0.6	-0.6	+8.6	-3.7	-5.5	-5.5

TABLE IV
Voltage Transformation Ratio against Primary Winding (P)

Windings	A	B	C	D	E	F
Ratios	1.781	1.780	1.779	1.780	1.780	1.781
Variation (%)	00	-0.05	-0.11	-0.05	-0.05	00

Tektronix DPO 2024 digital phosphor oscilloscope with P5200 high voltage differential probe and Tektronix TCPA300 current probe are used to observe waveforms. The voltage, current and their product (power) of primary windings are shown in Fig. 9 and the secondary A-windings voltage, current and power waveforms are shown in Fig. 10. Total power losses with respect to each winding for frequency range of 50 Hz to 12 kHz are measured. The losses are plotted over the frequency range of 50 Hz to 12 kHz. The loss characteristics of all windings are almost similar as shown in Figs. 11 and 12.

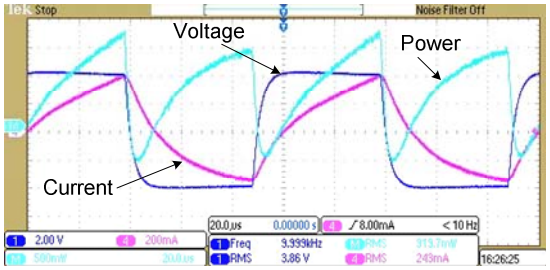

Fig. 9. P-windings voltage, current and power waveforms.

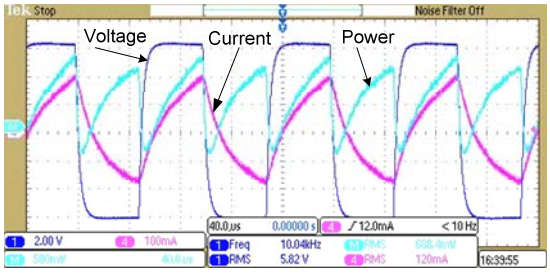

Fig. 10. A-windings voltage, current and power waveforms.

Different magnitude excitation currents are applied to all secondary windings separately. At 1 kHz excitation frequency all secondary windings show almost linear loss relations. The loss versus excitation current at 1 kHz excitation frequency is shown in Fig. 13. The losses at 10 kHz are much higher than those at 1 kHz. At 10 kHz, all secondary windings also show similar loss characteristics as in Fig. 14. Such similarity of characteristics is also important to generate balanced multiple sources for the SCHB system.

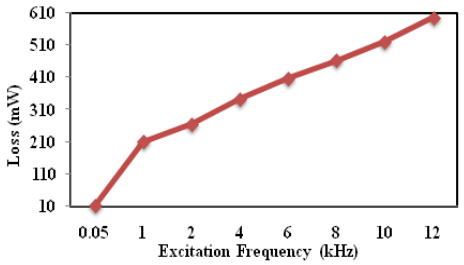

Fig. 11. P-windings loss versus frequency characteristics.

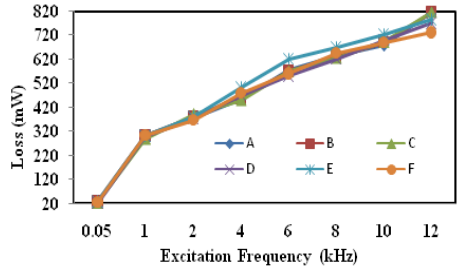

Fig. 12. Secondary windings loss versus frequency characteristics.

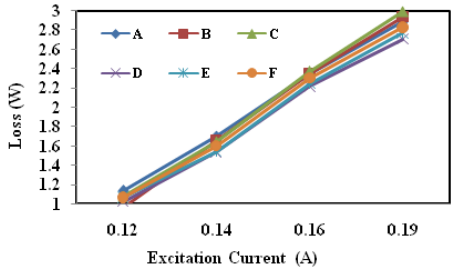

Fig. 13. Secondary windings loss characteristics at 1 kHz.

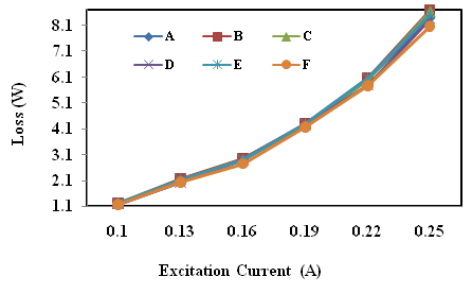

Fig. 14. Secondary windings loss characteristics at 10 kHz.

IV. Conclusions

A medium-frequency link is a possible solution to provide multiple isolated and balanced DC supplies and to overcome some fundamental drawbacks of the SCHB topology. This approach could be a feasible choice for medium-voltage converters for direct connection to the grid to eliminate the heavy and bulky step-up transformer, from the wind generation systems.

References

[1] ENERCON (May 2012), "E126/7500 stat of the art," [Online] Available at: http://www.enercon.de/en-en/66.htm

[2] ENERCON (June 2012), "Sway pushes ahead with 10 MW offshore/onshore turbine," [Online] Available at: http://www.swayturbine.no/publish_files/Sway_pushes_ahead_with_10_MW_offshore__onshore_turbine.pdf.

[3] AMSC (June 2012), "SeaTitan 10 MW wind turbine," [Online] Available at: http://www.amsc.com/documents/seatitan-10-mw-wind-turbine-data-sheet.

[4] AMSC (May 2012), "wt5500df and wt5500fc," [Online] Available at: http://www.amsc.com/documents/wt5500-data-sheet.

[5] Renewables International (April 2012), "Wind turbines, windenergieanlagen 2012," [Online] Available at: http://www.wind-turbine-market.de/pdf/WKA-Leseprobe_72dpi.pdf.

[6] GE Energy (June 2012), "GE 1.5 SLE turbine specifications," [Online] Available at: http://www.iprcanada.com/Plateau/PLATEAU%20FINAL%20ESR%20JUNE%2011%2009/AppendixG_Turbine-Specs.pdf.

[7] REpower Systems (May 2012), "Repower MM92, product description," [Online] Available at: https://www.edockets.state.mn.us/EFiling/edockets/searchDocuments.do?method=showPoup&documentId={7776F295-3DB6-4CD4-A0FE-1F8645A2081B}&documentTitle=20111-58786-01.

[8] ABB (June 2012), "Distribution transformer," [Online]. Available at: http://www.coronabd.com/download/ ABB%20Oil%20Distribution%20Transformer%20Catalogue.pdf.

[9] Pauwels. SLIM Transformer (April 2012), "SLIM transformer inside the world's highest wind turbine," [Online]. Available at: http://www.pauwels.com.

[10] J. S. Lai and F. Z. Peng, "Multilevel converters-a new breed of power converters", *IEEE Transactions on Industry Applications,* vol. 32, no. 3, pp. 509-517, 1996.

[11] A. Nabae, I. Takahashi and H. Akagi, "A new neutral-point-clamped PWM inverter", *IEEE Transactions on Industry Applications*, vol. 17, pp. 518-523, 1981.

[12] F. Z. Peng, J. S. Lai, J. McKeever and J. VanCoevering, "A multilevel voltage source inverter with separate DC sources for static VAR generation," *IEEE Transactions on Industry Applications*, vol. 32, no. 5, pp. 1130-1138, 1996.

[13] M. R. Islam, Y. Guo, J. G. Zhu and D. Dorrell, "Design and comparison of 11 kV multilevel voltage source converters for local grid based renewable energy systems," *Proc. of 37th Annual Conference of the IEEE Industrial Electronics Society (IECON 2011)*, Melbourne (Australia), Nov. 2011.

[14] M. R. Islam, Y. G. Guo and J. G. Zhu, "Performance and cost comparison of NPC, FC and SCHB multilevel converter topologies for high-voltage applications," *Proc. of 14th Int. Conf. on Electrical Machines and Systems*, Beijing (China), Aug. 2011.

[15] D. Zhong, B. Ozpineci, L. M. Tolbert, and J. N. Chiasson, "DC-AC cascaded H-bridge multilevel boost inverter with no inductors for electric/hybrid electric vehicle applications," *IEEE Transactions on Industrial Applications,* vol. 45, no. 3, pp. 963-970, May. 2009.

[16] S. S. Geun, K. F. Soon, and P. S. Jun, "Cascaded multilevel inverter employing three-phase transformers and single DC input," *IEEE Transactions on Industrial Electronics,* vol. 56, no. 6, pp. 2005-2014, 2009.

[17] J. Pereda and J. Dixon, "High-frequency link: a solution for using only one dc source in asymmetric cascaded multilevel inverters," *IEEE Transactions on Industrial Electronics,* vol. 58, no. 9, pp. 3884-3892, Sep. 2011.

[18] C. H. Ng, M. A. Parker, L. Ran, P. J. Tavner, J. R. Bumby and E. Spooner, "A multilevel modular converter for a large, light weight wind turbine generator," *IEEE Transactions on Power Electronics*, vol. 23, no. 3, pp. 1062-1074, May 2008.

[19] M. R. Islam, Y. Guo and J. G. Zhu, "H-bridge multilevel voltage source converter for direct grid connection of renewable energy systems," *Proc. of IEEE Power & Energy Society Innovative Smart Grid Technology Conference (ISGT 2011 Asia)*, Perth (Australia), Nov. 2011.